

# Review of Results from the Mark II Experiment at SLC\*

David P. Coupal  
representing the Mark II Collaboration

Stanford Linear Accelerator Center  
Stanford, California 94309

## Abstract

This paper reviews results on  $Z^0$  physics from the 1989 run of the Mark II experiment at the SLAC Linear Collider. Based on about  $20 \text{ nb}^{-1}$  we present results on the mass, width and branching ratios of the  $Z^0$  boson, the number of light neutrino species, properties of hadronic decays and searches for new particles.

## 1. Introduction

In the Standard Model the  $Z^0$  boson couples to all the fundamental fermions. Thus  $e^+e^-$  machines of sufficient energy to produce the  $Z^0$  boson provide excellent laboratories for studying the Standard Model, both the electroweak sector and QCD, and for searching for new particles or physics. The Mark II experiment at the SLAC Linear Collider is the first experiment to look at decays of the  $Z^0$  at one of these machines.

The SLAC Linear Collider is a single-pass collider that uses the linac to accelerate both electrons and positrons. Arcs at the end of the linac bend the beams around and a final set of optics focusses the beams down to a radius of 2-3 micron at the interaction point (IP). Most of the 1989 running was with a repetition rate of 60 Hz and bunch intensities of  $1-2 \times 10^{10}$  particles per bunch resulting in typical instantaneous luminosities of  $7 \times 10^{27} \text{ cm}^{-2} \text{ sec}^{-1}$ .

The Mark II detector is shown in Figure 1 and described in detail elsewhere<sup>[1]</sup>.

Invited talk presented at the APS Division of Particles and Fields  
General Meeting, Houston TX, January 3-6, 1990

---

\*Work supported in part by the Department of Energy contracts DE-AC03-81ER40050 (CIT), DE-AMOS-76SF00010 (UCSC), DE-AC02-86ER40253 (Colorado), DE-AC03-83ER40103 (Hawaii), DE-AC02-84ER40125 (Indiana), DE-AC03-76SF00098 (LBL), DE-AC02-76ER01112 (Michigan), and DE-AC03-76SF00515 (SLAC), and by the National Science Foundation (Johns Hopkins).

The vertex detectors were not installed for the 1989 running. A cylindrical central drift chamber (CDC) in a 4.75 kG solenoidal field provides charged particle tracking and particle identification using  $dE/dx$ . Outside the CDC are TOF counters, the magnet coil, and a lead/liquid Argon barrel calorimeter. The endcap regions are covered by a lead/proportional tube calorimeter. Muon counters outside the barrel calorimeter cover 45% of  $4\pi$ . A Small Angle Monitor (SAM) consisting of tracking and calorimetry provides low angle coverage and luminosity monitoring. A detector at small-

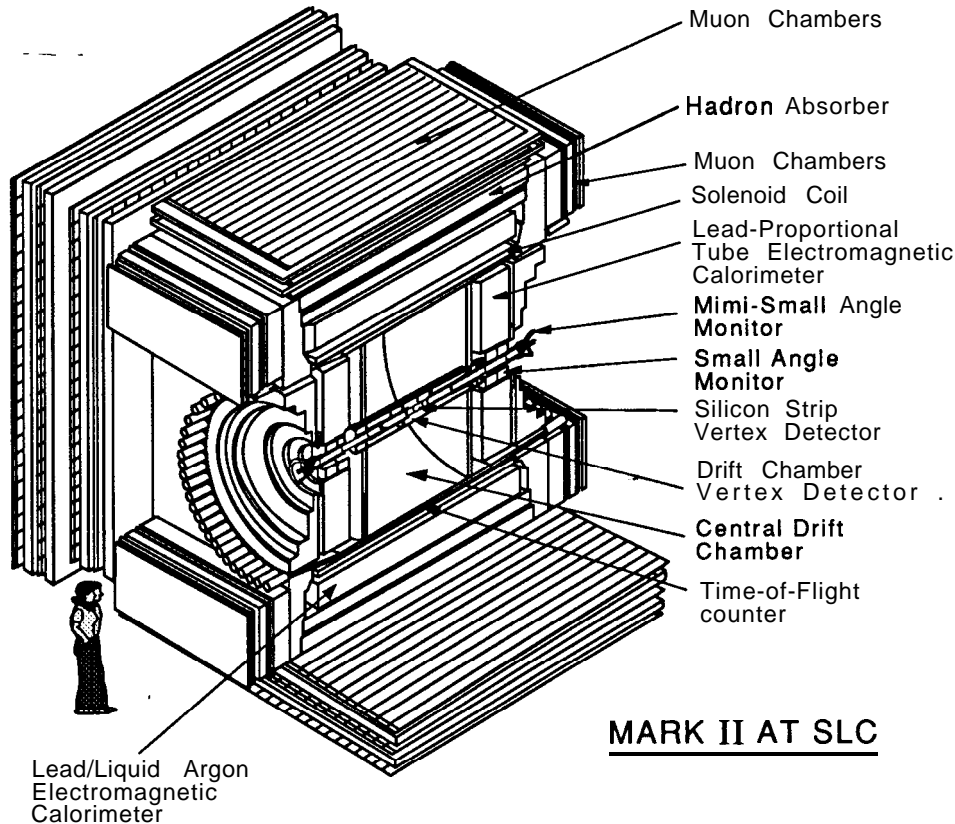


Figure 1. The Mark II Detector at SLC.

er angles (Mini-SAM) provides higher statistics luminosity monitoring. The central detector has a charged trigger that demands at least two tracks in the CDC and a calorimeter trigger that looks for clusters of energy deposition. Monte Carlo studies predict a combined trigger efficiency of over 99% for hadronic decays of the  $Z^0$ .

A measurement of the energies of both beams is critical for the  $Z^0$  mass and width determination. To this end, spectrometers measure the energy of each bunch on its way from the IP to their respective dumps. These spectrometers<sup>[2]</sup> measure the energies to an accuracy of 20 MeV. Possible position-energy correlations in the colliding beams add to the error in the center-of-mass energy ( $E_{cm}$ ) giving a total error of 35 MeV.

In the following we review Mark II results based on about  $20 \text{ nb}^{-1}$  of data collected between May and October of 1989. This sample corresponds to roughly 450 hadronic decays of the  $Z^0$ . The next section will briefly describe the data and subsequent sections present results on the  $Z^0$  mass and width, branching ratios, hadronic decays and new particle searches.

## **2. Data**

The 1989 data consists of a total of  $20 \text{ nb}^{-1}$  of data taken at 10 different values of  $E_{\text{cm}}$ . The sample consists of roughly 450 hadronic decays, 13  $\mu$  pairs, 21  $\tau$  pairs and 18 electron pairs.

Cuts on the data depend on the particular physics analysis but some of the same track quality cuts are used by most of the analyses presented here. Charged tracks are required to originate from a cylinder of radius 1 cm and half-length 3 cm centered on the IP. Charged tracking is efficient down to  $|\cos\theta| < .90$  but analyses that require good momentum measurement require  $|\cos\theta| < .82$ . Energy clusters in the calorimeters are required to be at least 1 GeV.

In the Monte Carlo detector simulation, particles from the desired physics process are tracked through the detector and used to generate fake raw data. This data is then mixed with real data from random beam crossings to simulate the beam-related backgrounds in the detector. The final mixed Monte Carlo data is submitted to the same analysis as the real data.

## **3. Mass, Width and Number of Neutrinos**

The mass of the  $Z^0$  boson ( $M_Z$ ) is a fundamental parameter of the Standard Model and its decay width ( $\Gamma_Z$ ) contains information on the number of particles that couple to the  $Z^0$  and the strength of those couplings.  $M_Z$  and  $\Gamma_Z$  can be determined by fitting the resonance in the decay rate  $\Gamma(e^+e^- \rightarrow Z^0 \rightarrow f)$  as a function of  $E_{\text{cm}}$ , where  $f$  is some final state.

Details of the Mark II analysis of the  $Z^0$  resonance can be found elsewhere<sup>[3]</sup>. We use for the final state,  $f$ , all hadronic  $Z$  decays and decays into  $\mu$  and  $\tau$  pairs. Hadronic event selection requires at least 3 charged tracks with  $|\cos\theta| < .90$  and at least  $.05 \times E_{\text{cm}}$  of energy visible in both the forward and backward hemispheres. Backgrounds from beam gas and two photon interactions are negligible. The efficiency, including the trigger, for hadronic decays is 95% as determined from Monte Carlo. The  $\mu$  and  $\tau$  pair events are required to have  $|\cos\theta_T| < .65$ , where  $\theta_T$  is the thrust angle. Restriction to this angular range insures high trigger efficiency and unambiguous identification.

The luminosity is measured at each value of  $E_{\text{cm}}$  using the SAM and Mini-SAM detectors described above. Bhabha scattering events into the SAM ( $50 < \theta < 160$  mrad) are selected by requiring 40% of the beam energy in each SAM. The overall normalization is done to a smaller fiducial volume ( $60 < \theta < 160$  mrad) with an accurately cal-

culable cross section. The Bhabha cross section into this region is 25.2 nb at 91.1 GeV. The estimated systematic errors are 2% from unknown higher order radiative corrections and 2% due to detector resolution and reconstruction. The selection of Bhabha events in the Mini-SAM involves looking for back-to-back showers in pairs of quadrants. The overall cross section is determined by normalizing to the SAM giving 227 nb at  $E_{\text{cm}}=91.1$  GeV (234 nb for the last 3 scan points following a detector realignment).

Figure 2 shows the resulting resonance shape in the cross section versus  $E_{\text{cm}}$ . The data are fitted to a relativistic Breit-Wigner of the form:

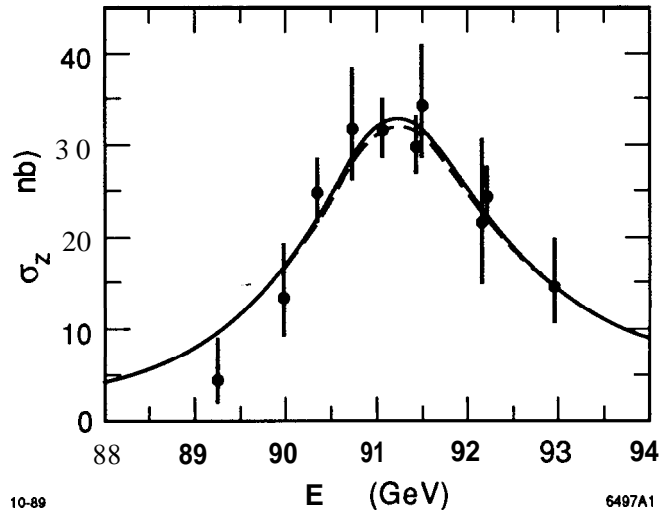
$$\sigma_z(E) = \frac{s\Gamma_e\Gamma_f}{M_Z^2(s - M_Z^2)^2 + s^2\Gamma^2/M_Z^2}(1 + \delta(E))$$

where  $s=E_{\text{cm}}^2$ ,  $\delta$  is an analytical approximation of the radiative corrections<sup>[4]</sup>,  $\Gamma_e$  is

the electron partial width, and  $\Gamma_f$  is the partial width for decays into our fiducial volume.  $\Gamma_f$  is given in terms of the hadronic,  $\mu$  and  $\tau$  partial widths by  $\Gamma_f = \Gamma_h + f(\Gamma_\mu + \Gamma_\tau)$  where  $f=0.556$  is the fraction of  $\mu$  and  $\tau$  events with  $|\cos\theta_T| < 0.65$ . The total  $Z$  width,  $\Gamma$ , is given by

$\Gamma = \Gamma_h + \Gamma_e + \Gamma_\mu + \Gamma_\tau + N_\nu \times \Gamma_\nu$ , where  $N_\nu$  is the number of light neutrino families.

Three fits are done to the data in Figure 2. The first fit varies only the mass ( $M_Z$ ), the second fit allows the mass and number of neutrinos to vary and the third fit allows the mass, total width and peak cross section ( $\sigma_0$ ) to vary. The results are shown in Table 1. The result for  $N_\nu$  can be translated into a 95% CL upper limit of  $N_\nu < 3.9$ , excluding to this level a



10-89

6497A1

Figure 2.  $e^+e^-$  annihilation cross sections to hadronic events plus  $\mu$  and  $\tau$  pairs with  $|\cos\theta_T| < 0.65$ . The dashed curve represents the result of the first fit and the solid curve the second and third fits, which are indistinguishable.

Table 1. Results of fit to $Z^0$ resonance.				
Fit	$M_Z$ GeV/c <sup>2</sup>	$N_\nu$	$\Gamma$ GeV	$\sigma_0$ nb
1	91.14f0.12	--	--	--
2	91.14f0.12	2.8k0.6	--	--
3	91.14±0.12	--	2.42+.45-.35	45±4

fourth light neutrino specie. The fits for  $\Gamma$  and  $\sigma_0$  should be compared to the Standard Model predictions of 2.45 GeV and 43.6 nb respectively.

#### 4. Branching Ratios

The Standard Model makes definite predictions of the couplings of the  $Z^0$  to the fermions. It predicts for the ratio of the decay rate into a pair of leptons to the rate into hadrons to be  $\Gamma(Z^0 \rightarrow \ell^+ \ell^-) / \Gamma(Z^0 \rightarrow \text{hadrons}) = .048$ . To separate the different leptonic decay modes, the calorimetry is used to distinguish electron and muon events and a cut on the minimum momentum of the 2 tracks is used to separate 1-1 topology  $\tau$  decays from the electron and  $\mu$  events. After correcting the electron sample for the presence of Bhabha events we get  $\Gamma_{ee} / \Gamma_{\text{had}} = .037^{+.016}_{-.012}$ ,  $\Gamma_{\mu\mu} / \Gamma_{\text{had}} = .053^{+.020}_{-.015}$ , and  $\Gamma_{\tau\tau} / \Gamma_{\text{had}} = .066^{+.021}_{-.017}$  in good agreement with the Standard Model. Details of this analysis can be found elsewhere<sup>[5]</sup>.

We have also measured the branching ratio of  $Z^0$  into bottom quarks<sup>[6]</sup>. In this analysis we use the semileptonic decay of the b quark. For electrons and muons with momentum greater than 2 GeV, Figure 3 shows the  $p_T$  relative to the closest jet. Electrons are identified in the calorimetry and muons in the muon counters. Counting the number of events containing a tagged lepton with  $p_T$  greater than 1.25 GeV/c and correcting for background and acceptance gives  $\Gamma_{bb} / \Gamma_{\text{had}} = .23^{+.11}_{-.09}$ , in agreement with the Standard Model value of .22.

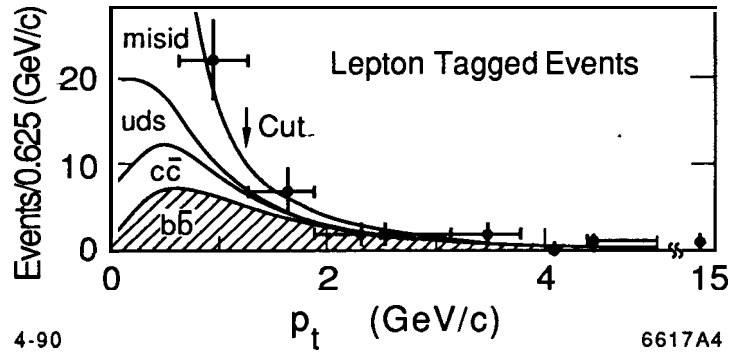


Figure 3.  $p_T$  distribution for tracks tagged as electrons or muons with the Monte Carlo prediction of the different contributions.

#### 5. Hadronic Decays

In the Standard Model hadronic decays are 70% of the available decay modes, providing a clean environment for high statistics studies of QCD. We review Mark II results on global shape parameters<sup>[7]</sup>, which are sensitive to parton level processes, and inclusive particle distributions<sup>[8]</sup>, which give insight into the fragmentation process. Fragmentation models used in the comparisons include the Lund 6.3<sup>[9]</sup>, the Webber 4.1<sup>[10]</sup>, and the Caltech II 86<sup>[11]</sup> parton shower models and a Lund model based on a second order QCD matrix element calculation by Gottschalk and Shatz<sup>[9,12]</sup>. The parameters of these models were tuned to fit the Mark II data taken at PEP at  $E_{\text{cm}}$

= 29 GeV. We also present the first measurement of  $\alpha_s$  at this higher  $q^2$  and compare to a measurement done at PEP with the same detector and technique<sup>[13]</sup>.

Event selection cuts include the demand that the event have at least 7 tracks and that the visible energy be at least 50% of  $E_{cm}$ . These cuts insure that the background is low and the event is well contained within the detector. The efficiency as determined from Monte Carlo is  $78 \pm 2\%$ .

Common global shape parameters used in many analyses are thrust, sphericity and aplanarity. Figure 4 shows one of these variables, sphericity, compared to the 4 models. The mean values of the quantities (corrected for detector effects) are shown in Figure 5 as a function of  $E_{cm}$  and compared to other measurements at lower energy and with the Lund parton shower prediction. Also shown in Figure 5 is the fraction of 3-jet events, where jets are found using the standard JADE algorithm with  $y_{cut} = .08$ .

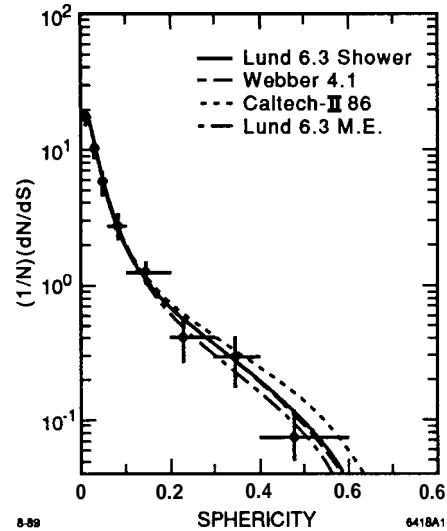


Figure 4. Sphericity distribution for hadronic decays of the  $Z^0$ .

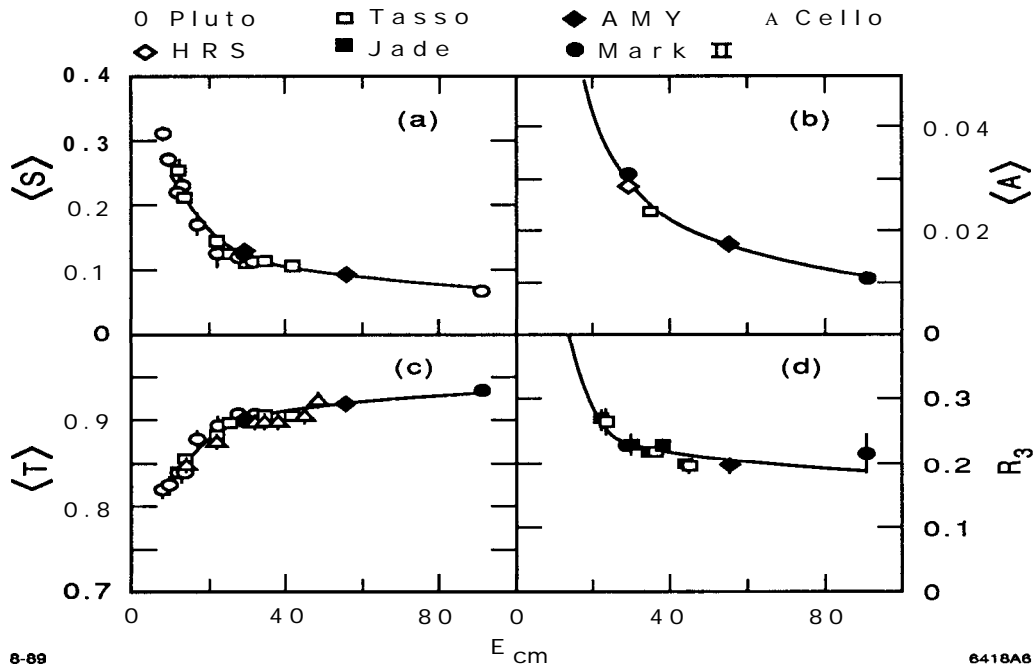


Figure 5. Corrected mean sphericity, aplanarity, thrust and 3-jet fraction versus  $E_{cm}$ . The solid curve is the prediction from the Lund parton shower model.

Fragmentation models can be studied by looking at charged particle inclusive distributions. The corrected mean charged multiplicity was found to be  $20.1 \pm 1.2$ . Figure 7(a) shows the corrected charged particle inclusive distribution in the scaled momentum  $x = 2p/E_{cm}$ . Figure 7(b) shows it versus  $E_{cm}$  for several  $x$  bins together

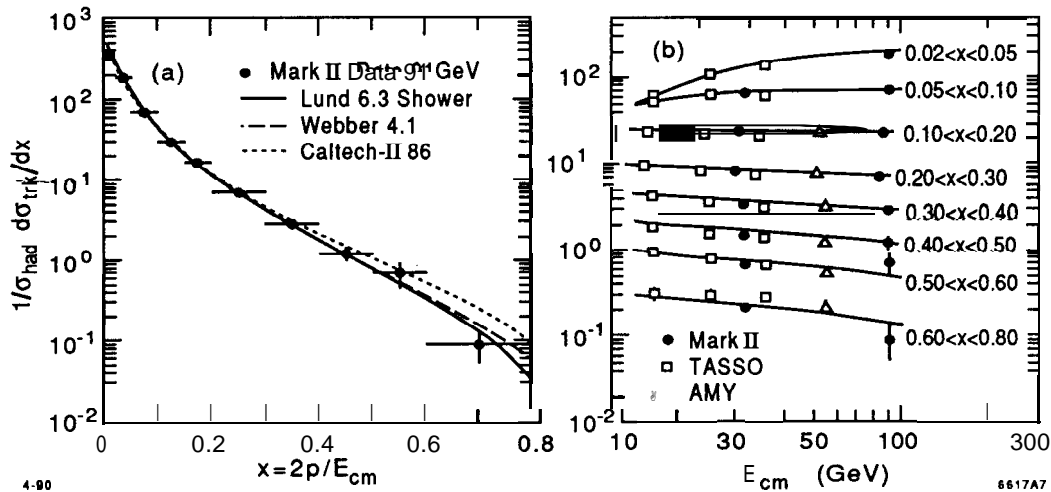


Figure 7. (a) Inclusive  $x$  distribution for hadronic decays compared to parton shower models. (b) Inclusive distribution versus  $E_{cm}$  in  $x$  bins. The solid lines are the Lund model prediction.

with  $e^+e^-$  data at lower  $E_{cm}$ . The mean of the square of the momentum transverse to the sphericity axis both in the event plane ( $p_{\perp in}$ ) and out of the event plane ( $p_{\perp out}$ ) is shown in Figure 8. These data are compared to Mark II data from PEP, data from other experiments and the Lund model.

The strong coupling constant,  $\alpha_S$ , is a fundamental parameter of QCD. We have measured  $\alpha_S$  by fitting the distribution of differential jet multiplicity versus the value of  $y_{cut}$ . This technique has been applied to Mark II PEP data taken at  $E_{cm} = 29$  GeV and again at the SLC with  $E_{cm} = 91.1$ . Choosing the renormalization point at  $q^2 = E_{cm}^2$  gives  $\alpha_S = 0.123 \pm 0.009 \pm 0.005$  at SLC and  $\alpha_S = 0.149 \pm 0.002 \pm 0.007$  at PEP in good agreement with the QCD prediction of the running of  $\alpha_S$  with  $q^2$ .

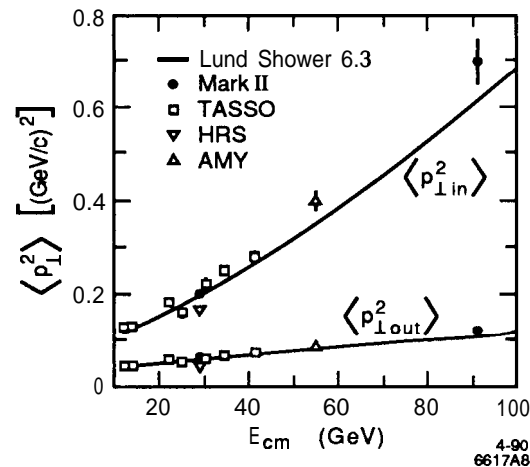


Figure 8. Mean values of  $p_{\perp in}^2$  and  $p_{\perp out}^2$  vs  $E_{cm}$  for various experiments.

## 6. Search For New Particles

The new energy regime opened up by the SLC makes it natural to look for the

production of new particles, in particular heavier equivalents of the known fermions such as the top or  $b'$  quark or a heavy neutrino. A fourth light neutrino has already been eliminated by the measurement of the  $Z^0$  resonance. We review below limits on the mass of the top and  $b'$  quarks using an isolated track and event shape analysis<sup>[14]</sup>. We also present limits on heavy neutrinos using the isolated track analysis<sup>[14]</sup>, search for displaced vertices<sup>[15]</sup> and a search for jets containing 2 tracks consistent with a heavy neutrino decaying into  $\tau\ell^\pm\nu_\ell$ <sup>[16]</sup>.

The isolated track analysis uses the fact that semileptonic decays of heavy quarks will tend to produce tracks well isolated from the jet coming from the secondary quark. We define a parameter  $\rho_{track} = \{2E(1-\cos\theta_{jet})\}^{1/2}$  where  $\theta_{jet}$  is the angle to the nearest jet and define  $\rho$  for the event as the maximum of all the  $\rho_{track}$ . A cut of  $\rho > 1.8$  is used to select top or  $b'$  events. We observe one event with  $\rho > 1.8$  in our sample of  $Z^0$  hadronic decays. The expected background varies from .9 to 1.8 events depending on the fragmentation model. To be conservative we assume the smallest value (.9 events) and can set limits of  $M_{top} > 40.0$  and  $M_{b'} > 44.7 \text{ GeV}/c^2$ .

A similar analysis can be done looking for the non-leptonic 4-jet decays for the heavy quarks. We define the quantity

$$M_{out} = \frac{E_{cm}}{E_{vis}} \frac{1}{c} \sum |p_{T_i}^{out}|$$

where  $p_t^{out}$  is the momentum transverse to the event plane. A cut of  $M_{out} > 18 \text{ GeV}/c^2$  is used to select heavy quark decays. This selection is also sensitive to heavy quark decays involving charged Higgs ( $t \rightarrow H^+b$ ,  $b' \rightarrow H^+c$ ). We find 6 events with  $M_{out} > 18$  and expect 4.8-11.7 depending on the model. Again taking the most conservative (4.8 events) we can set the limits  $M_t > 40.7$  and  $M_{b'} > 44.2 \text{ GeV}/c$ . If the dominant decay mode is through a charged Higgs ( $M(H^\pm) > 25 \text{ GeV}$ ) then the limits are  $M_t > 42.5$  and  $M_{b'} > 45.2 \text{ GeV}/c^2$ .

As already discussed above the measurement of the  $Z^0$  resonance shape rules out the existence of a light 4<sup>th</sup> generation neutrino. This limit excludes stable neutrino masses up to about  $19 \text{ GeV}/c^2$ . The phase-space suppression in the production of heavier neutrinos limits the sensitivity to higher masses. Direct searches are possible provided the heavy neutrino decays by some mechanism. Barring the existence of a charged partner lighter than the massive neutrino, a common mechanism of generating a massive unstable neutrino is through mixing with the lighter neutrinos. Just as in the quark sector, the mass eigenstate,  $\nu_4$ , may be a mixture of the weak eigenstates,  $\nu_\ell$  ( $\ell=e,\mu,\tau,L$ ) so that

$$\nu_\ell = \sum_{i=1}^4 U_{\ell i} \nu_i$$

leading to decay rates of  $\nu_4 \rightarrow \ell^\pm + W^*$  dependent on  $|U_{\ell 4}|^2$ .

For short-lived decays (large  $|U_{\ell 4}|^2$ ) the isolated track analysis can be used to set limits assuming Standard Model coupling to the  $Z^0$ . Figure 9 shows the limits of



$M(\nu_4)$  vs  $|U_{\ell 4}|^2$  from this analysis for  $\ell = e, \mu$  and  $\tau$ .

Smaller values of  $|U_{\ell 4}|^2$  imply a long-lived neutrino and therefore the decays may be displaced from the interaction point. We looked for displaced decay vertices by looking at the impact parameter of the charged tracks in an event. Figure 9 shows

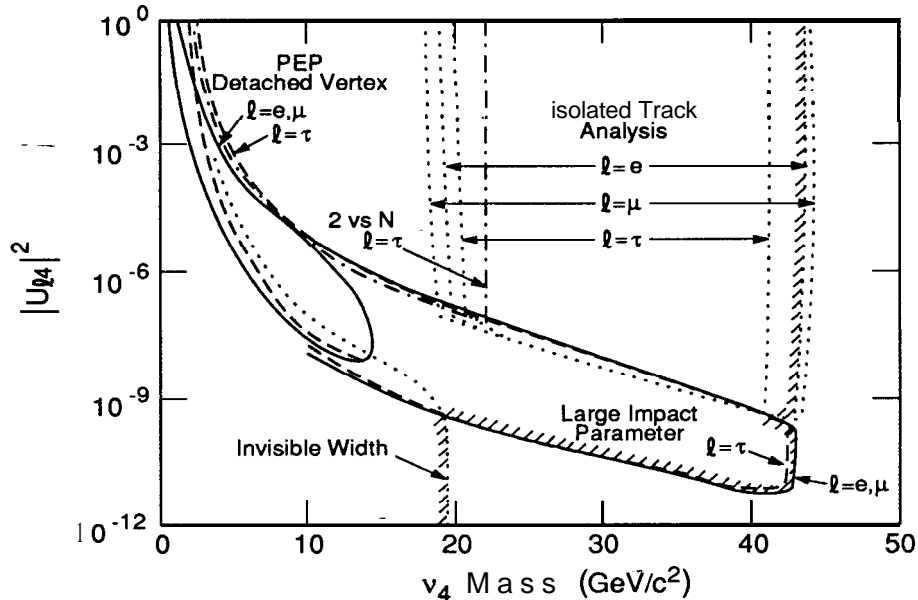


Figure 9. 95% C. L. excluded regions for a 4th generation massive Dirac neutrino as a function of mass and mixing. The analyses used in the different limits are described in the text. The hatched line shows the combined limit for  $\ell = e$ .

the limits from this analysis along with the limits from the search for detached vertices at PEP. Finally, Figure 9 also shows the limit between masses of 2.2 and 20  $\text{GeV}/c^2$  derived from a search for events where one heavy lepton decays via  $\nu_4 \rightarrow \tau \ell^\pm \nu_\ell$  and the other decays hadronically (2 vs N).

## 7. Conclusions

Based on a sample of roughly 500  $Z^0$  decays, the Mark II experiment has been able to measure the mass of the  $Z^0$  to 120 MeV, eliminate the existence of a 4<sup>th</sup> generation light neutrino at the 95%CL and confirm the Standard Model in the leptonic and hadronic decays. We have also set limits on the existence of the top and  $b'$  quark and a massive neutrino decaying through mixing to lighter neutrinos.

The Mark II has installed silicon strip and drift chamber vertex detectors. We will take data again in the Summer of 1990 during which we hope to log an additional 3-4 k  $Z^0$  decays.

## REFERENCES

- [1] G. Abrams et al., **Nucl. Instrum. Methods A** **281**, 55 (1989).
- [2] J. Kent et al., SLAC-PUB-4922 (1989); M. Levi, J. Nash, and S. Watson, **Nucl. Instrum. Methods** **A281,265** (1989); M. Levi *et al.*, SLAC-PUB-4921 (1989).
- [3] B. Harral, these proceedings; G. S. Abrams *et al.*, **Phys. Rev. Lett.** 63 2173 (1989).
- [4] R. N. Cahn, **Phys. Rev. D** **36**, 2666 (1987). Eqs. 4.4 and 3.1 .
- [5] M. Kuhlen, these proceedings; G. S. Abrams *et al.*, **Phys. Rev. Lett.** **63**, 2780 (1989).
- [6] J. F. Kral, these proceedings; J. F. Kral *et al.*, **Phys. Rev. Lett.** 64, 1211 (1990).
- [7] E. Wicklund, these proceedings; G. S. Abrams *et al.*, **Phys. Rev. Lett.** 63 (1989).
- [8] K. O'Shaughnessy, these proceedings; G. S. Abrams *et al.*, **Phys. Rev. Lett.** 64 1334 (1990).
- [9] T. Sjostrand, **Comput. Phys. Commun.** 39,347 (1986); T. Sjostrand and M Bengtsson, **Comput. Phys. Commun.** 43,367 (1987); M. Bengtsson and T. Sjostrand, **Nucl. Phys.** **B289**, 810 (1987).
- [10] G. Marchesini and B. R. Webber, **Nucl. Phys.** **B238**, 1 (1984); B.R. Webber, **Nucl Phys.** B238, 492 (1984).
- [11] T. D. Gottschalk and D. Morris, **Nucl. Phys.** **B288**, 729 (1987).
- [12] T. D. Gottschalk and M. P. Shatz, **Phys. Lett.** **150B**, 451 (1985); CALTECH Report No. CALT-68-1 172, -1173, -1 199.1985 (unpublished); T. D. Gottschalk (private communication).
- [13] S. Komamiya, these proceedings; S. Komamiya, *et al.*, **Phys. Rev. Lett.** 64,987 (1990).
- [14] R. Van Kooten, C. K. Jung, and S. Komamiya, these proceedings; G. S. Abrams *et al.*, **Phys. Rev. Lett.** **63**, 2447 (1989).
- [15] R. Van Kooten, C. K. Jung, and S Komamiya, these proceedings; C. K. Jung *et al.*, **Phys. Rev. Lett.** **64**, 1091 (1990).
- [16] R. Van Kooten, C. K. Jung and S Komamiya, these proceedings; P. R. Burchat *et al.*, SLAC-PUB-5172, LBL-28458 (Jan 1990), (Submitted to **Phys. Rev. Lett.**)